

BIOMIMETIC TRANSFEMORAL KNEE WITH A GEAR MESH LOCKING MECHANISM

Tyagi Ramakrishnan, University of South Florida; Millicent Schlafly, University of South Florida;
Kyle B. Reed, University of South Florida

Abstract

The innovation presented in this paper is a passive knee locking mechanism that incorporates a cross-linked, four-bar mechanism similar to the sagittal plane configuration of the anterior cruciate ligament (ACL) and posterior cruciate ligament (PCL). The flexible four-bar mechanism guides the motion of the knee and aids in the return of the knee from full flexion to extension. The flexible four-bar mechanism also connects the femoral spur gear to the tibia spur gear. The gears are based on a circular radius, derived from femoral condyle dimensions. The gears are connected using a parallel link to keep the femur and tibia from moving away from each other when the knee is in motion. This prosthetic knee design is based on the anatomical dimensions of a human knee, which allows the design to be scaled from a large adult male to a small pediatric knee.

Introduction

Human gait consists of a synchronized and cyclic movement of each leg that helps a person move forward [1]. Walking is a complex and coordinated process that recruits a range of muscles to actuate the motion. This coordination is disrupted by a limb amputation. The knee and ankle joints are a vital part of human locomotion and are responsible for articulation, load bearing, and the general dynamic control of an overall stable gait [2]. Therefore, an amputation that causes a loss of either joint is detrimental to a person's gait [3]. Improving the design of prostheses can greatly increase the quality of life of a person with an amputation by increasing their potential mobility. There are about seven million transfemoral amputees around the world [4], and each amputee is unique and, hence, requires a custom prosthesis. With the advent of 3D printing technology on the rise, it is becoming possible to customize a prosthesis to a specific individual's size and gait pattern [5]. It is also possible to tailor-make a prosthesis that has anatomically similar dimensions to the person, while making the design inexpensive and passive.

Current prosthetic knees are either passive or active mechanisms [6, 7]. Active knee mechanisms are considered state-of-the-art and the designs incorporate complex mechanisms that enable the actuators to mimic human walking [5]. Active knee mechanisms cause more lower metabolic strain

than passive knees in tasks such as walking, stair ascent, traversing slopes, and ambulatory tasks [3, 8, 9]. Active knees use variable control algorithms to adjust for terrain and environmental conditions. However, active knees are expensive, and transfemoral amputees typically use their passive knees more than their active knees [10]. Also, additional training is required to properly fit and fine-tune active knees, which hinders the widespread adoption of active knees [11].

The human knee is categorized as a condylar joint. It can be closely represented by a polycentric mechanism. Polycentric mechanisms are one of the five forms of passive knee mechanisms: manual, single axis, weight activated, polycentric, and knee with exterior hinges [12, 13]. The knees are designed to assist amputees with various control levels given by the K level (K is an arbitrary letter assigned by HCFA) [13, 14]. Low-control amputees of the scale K0-K2 rely on manual locking mechanisms. The manual locking knee relies on user input to lock and unlock the knee joint during gait, thereby giving full control to the user. The widely used polycentric knees are for a user with medium to high control [15]. A four-, five-, or six-bar mechanism [12, 16] can be used for a polycentric knee. These mechanisms shift the instantaneous center throughout the gait cycle to improve locking and unlocking of the knee joint. Other mechanisms, such as a single-axis knee, are used in conjunction with hydraulic or weight-activated locking systems to aid in the control and return to extension [13]. This biomimetic knee design uses a polycentric, cross-linked four-bar mechanism that is designed to mimic the anatomical movement of the human knee. This knee design can be tuned to offer a wide range of control from K0 to K4.

There have been several attempts to recreate the human knee joint in a prosthetic mechanism. Figure 1 (a1-c1) shows the ACL and PCL, which play an integral part of knee kinematics, are modeled as a cross-linked four-bar mechanism [17-20]. Anatomically, the mechanism consists of the femur, tibia, ACL, and PCL. The simplistic representation as a four-bar mechanism excludes the fact that the knee joint is controlled by several muscles to execute refined motion [21]. It only focuses on the sagittal plane kinematics. The knee joint rolls, slides, and rotates as it goes from extension to flexion, which is called knee roll back [22]. This motion is controlled by the ACL and PCL that stabilize the knee at every position. A tear in either ligament

causes detrimental effects to the motion of the knee, which in turn greatly affects a person's gait [23].

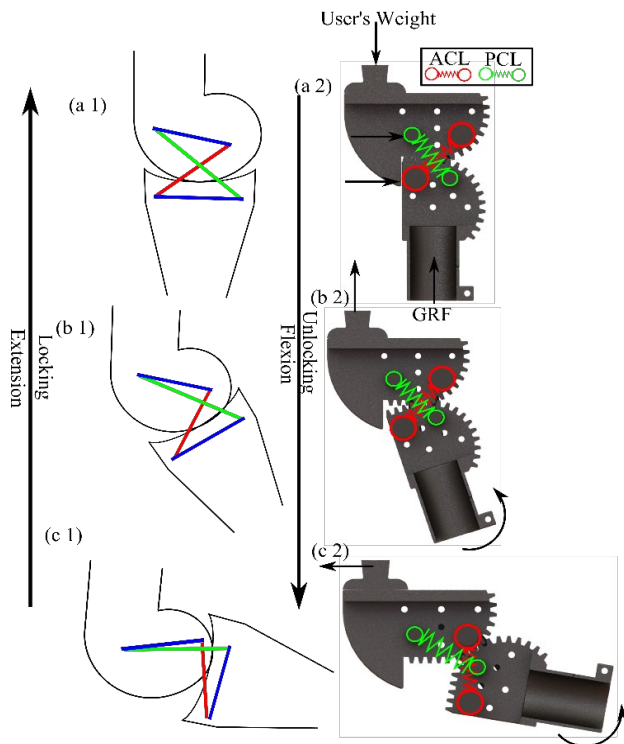


Figure 1. Comparison of Human (a1-c1) and Biomimetic (a2-c2) Knee Motions

There is also a need for prosthetics to be unique to every amputee's condition. Current prosthetic products are designed to be of similar dimensions, due to manufacturing, design, and cost constraints. Fitting prostheses that are not suitable to the user's dimensions causes an array of problems with their gait dynamics, which in turn leads to physical pain. The mechanism detailed in this paper bridges the gap of anatomically similar prostheses and scaling the design with the dimensions of the amputee limb. This customization can be easily achieved with additive manufacturing. The prosthetic design presented here can be made available in a way such that a person with access to a 3D printer can make a viable product, thereby driving down the cost of manufacturing.

Design

Figure 2 shows how the knee design consists of four major components: femur gear, tibia gear, spring holders, and outer linkages. The femur and tibia gears are modified to aid in locking the knee. The circular gear ends with a flat rack on both gears that absorb the load during weight bearing and prevents hyperextension. The radius of the circular gear

can be scaled to fit any amputee's anatomical femoral dimension. The spring holders can be fit with a range of springs that vary in stiffness, depending on the control level of the amputee. There are also other holes provided on the femur and tibia that allow for different configurations of initial spring stiffness to better aid in the dynamics of the knee joint. The outer links provide lateral support and keep the knee mechanism intact. Depending on the configuration of the springs, they can act as returning and stabilizing mechanisms.

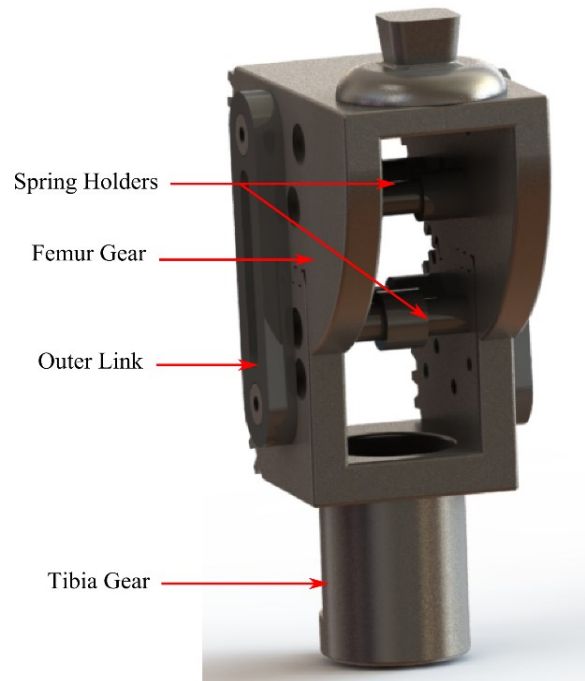


Figure 2. Parts of the Knee Mechanism

The function of the knee is straightforward, and Figure 1 (a1-c2) shows how the kinematics of the mechanism were designed to mimic the human knee. When the user's weight is applied to the top of the femoral spur gear, it locks with the tibia spur gear. The weight of the user is applied towards the anterior of the femoral spur gear in order to prevent buckling of the knee. The knee stays locked throughout the stance phase. At toe-off, the weight of the user shifts to their opposite leg and no weight is applied to the prosthetic knee. This shifting of weight allows the knee to flex and is guided by the four-bar mechanism that behaves like the ACL and PCL in a normal knee. In essence, the flexible links are stretched to a certain length, thereby increasing the force from the springs. Figure 3 (a-f) shows how, at terminal swing phase, just before heel strike, the flexible links in the four-bar mechanism snap back to the extended locked position and lock completely once the user applies weight on the knee.

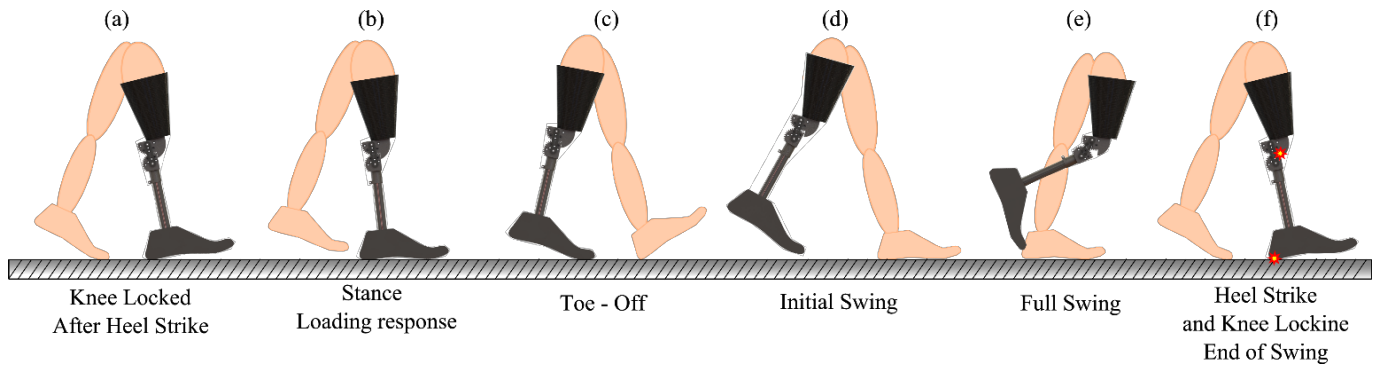


Figure 3. Gait with the Prosthetic Knee

This knee prosthesis has very few parts, and thus is a good candidate for sustainable additive manufacturing, which can offer the highly customized products needed by amputees. The prototypes used for this study were made of 3D-printed ABS and nylon. Functional pediatric knees can be made out of these materials and the child amputee can get a new knee when they outgrow their old. It is also a viable candidate to be produced using metal additive manufacturing processes for adult sizes, when added strength is needed. An MRI image of the amputee's intact femur can be used to obtain the pitch diameter of the gear used in the prosthetic knee mechanism. In case of bilateral amputees, a person of similar proportion can be used for sizing purposes. The pitch diameter of the gear will be twice the average radius of the femoral condyles. Femoral condyles radii generally range from 20–30 mm for adults [24-27]. The pitch radius used for this design was 28.5 mm, which is on the larger side of the condylar radii range, because the kinematics match better.

Table 1 shows the gear design parameters for two different sizes. The femur and tibia spur gear have the same gear pitch diameter. This versatility and biomimetic design make this knee unique and highly customizable. The knee also facilitates modification to add control elements that can benefit amputees with lower control, since it operates using simple spur gears and springs. For example, a high-functioning amputee may desire low stiffness for an instantaneous response from the knee and a lower functioning amputee may require higher stiffness for more control. The specific cross-linked four-bar mechanism used for this design, represented in Figure 4, was designed similar to the anatomical mechanism consisting of the ACL and PCL, as described from the sagittal plane. The mechanism presented here has slightly different dimensions to simplify the design and make it easier to model. The mechanism consists of two pivot points that can be seen as P_1 and P_2 in Figure 4(a). P_1 is the pivoting joint at the Femur and P_2 is the pivoting joint for the Tibia. The blue link represents the shank and is perpendicular to link c-d.

Table 1. Gear Design Parameters for Different Sizes

| Gear parameter | Adult | Child (assuming half the size) |
|--------------------------------|---------|--------------------------------|
| Pitch radius (Condylar radius) | 28.5 mm | 14.25 mm |
| Teeth pressure angle | 14.5° | 14.5° |
| Number of teeth in full gear | 25 | 25 |
| Number of teeth in the rack | 4 | 4 |
| Addendum | 1.14 | 0.57 |
| Diametric pitch | 0.877 | 1.754 |
| Module | 1.14 | 0.57 |
| Velocity ratio | 1 | 1 |

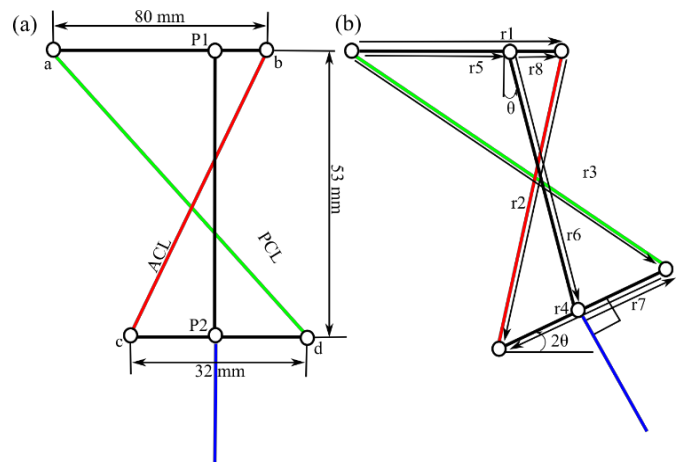


Figure 4. Prosthetic Knee Mechanism (a) Dimensions and (b) Vectors

The analysis of the four-bar mechanism was performed using position vector-based equations. Figure 4(b) shows the vector representation and consists of five vectors, one for each link, and three smaller vectors defining a section of

a link. The constraints applied to this mechanism are that vectors $r_1, r_4, r_5, r_6, r_7,$ and r_8 are of a fixed length, while vectors r_3 and r_2 represent the springs in the design and are allowed to change in length, as shown in Table 2. Another constraint is that r_4 is constrained to move twice the angle of r_6 , which is imposed by the gear and four-bar mechanism configuration.

Table 2. Position Equation Parameters

| | |
|------------------------|----------------------------|
| $r_1 = 80$ mm | $\theta_1 = 0$ |
| $r_4 = 32$ mm | $\theta_4 = 180 + 2\theta$ |
| $r_5 = 60$ mm | $\theta_5 = 0$ |
| $r_8 = 20$ mm | $\theta_8 = 0$ |
| $r_6 = 53$ mm | $\theta_6 = 170 + \theta$ |
| $r_7 = 0.5 * r_4 = 16$ | $\theta_7 = 2\theta$ |

Equations (1)-(10) were solved using Matlab to obtain the positions of the moving links and joints. Some variables were fixed to constrain the size of the design. Solving Equations (1)-(4) or Equations (3)-(6) will give the solutions for the four unknown variables, which are $r_2, r_3, \theta_1,$ and θ_2 . Figure 5 shows the motion of the mechanism with the given inputs for a flexion from 0° to 90° , where P_1 and link a-b are fixed. Figure 6 shows how the ACL and PCL change in length with respect to the corresponding flexion angle. The change of prosthetic ACL and PCL link length was compared to the change of length of the ACL and PCL ligament obtained from anatomical data [28]. Figure 6 shows that this prosthetic knee mechanism has the potential to exhibit biomimetic behavior with respect to the ACL and PCL behavior of the anatomical data [28].

$$r_1 \cos(\theta_1) + r_2 \cos(\theta_2) = r_3 \cos(\theta_3) + r_4 \cos(\theta_4) \quad (1)$$

$$r_1 \sin(\theta_1) + r_2 \sin(\theta_2) = r_3 \sin(\theta_3) + r_4 \sin(\theta_4) \quad (2)$$

$$r_5 \cos(\theta_5) + r_6 \cos(\theta_6) + r_7 \cos(\theta_7) = r_3 \cos(\theta_3) \quad (3)$$

$$r_5 \sin(\theta_5) + r_6 \sin(\theta_6) + r_7 \sin(\theta_7) = r_3 \sin(\theta_3) \quad (4)$$

$$r_8 \cos(\theta_8) + r_2 \cos(\theta_2) + r_7 \cos(\theta_7) = r_6 \cos(\theta_6) \quad (5)$$

$$r_8 \sin(\theta_8) + r_2 \sin(\theta_2) + r_7 \sin(\theta_7) = r_6 \sin(\theta_6) \quad (6)$$

$$\dot{r}_2 = \dot{\theta} (r_6 \sin(\theta_6 - \theta_2) - 2r_7 \sin(\theta_7 - \theta_2)) \quad (7)$$

$$\omega_2 = -\frac{\dot{\theta}}{r_2} (r_6 \cos(\theta_6 - \theta_2) + 2r_7 \cos(\theta_7 - \theta_2)) \quad (8)$$

$$\dot{r}_3 = -\dot{\theta} (r_6 \sin(\theta_6 - \theta_3) + 2r_7 \sin(\theta_7 - \theta_3)) \quad (9)$$

$$\omega_3 = \frac{\dot{\theta}}{r_3} (r_6 \cos(\theta_6 - \theta_3) + 2r_7 \cos(\theta_7 - \theta_3)) \quad (10)$$

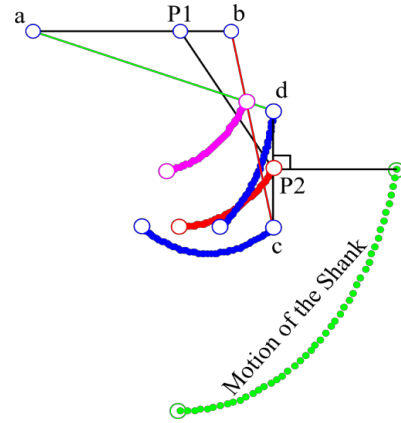


Figure 5. The Motion of the Mechanism

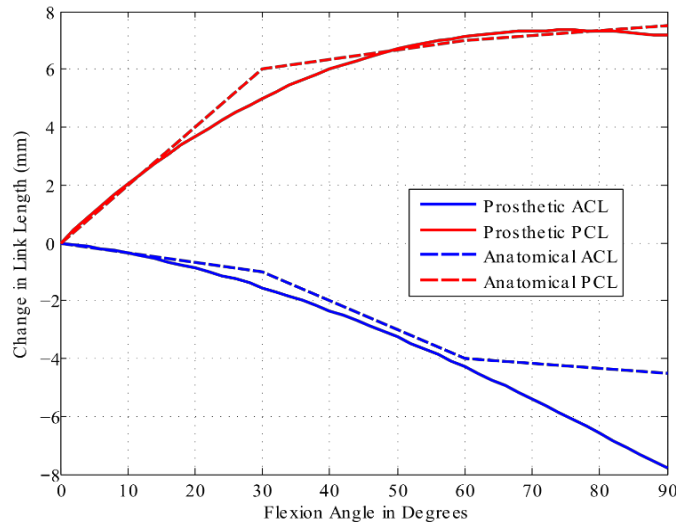


Figure 6. Changes in Length of ACL and PCL

The linear and angular velocity equations for change in length of ACL (r_2) and PCL (r_3) are defined in Equations (7)-(10). Figure 7 is a plot of the resultant linear velocities, where a constant velocity of 10 rad/s was assumed, as it is reported to the peak angular velocity during gait [29]. The rate of change of PCL length decreases as the knee approaches full flexion. This is compensated by the ACL, which changes length at a more rapid frequency as the knee is in flexion. Figure 8 shows the angular velocity of the rate of change of the angles that ACL (θ_2) and PCL (θ_3) make with the positive x-axis changes over flexion. While there is a negative change in angular velocity for the ACL, it is a positive change for the PCL link.

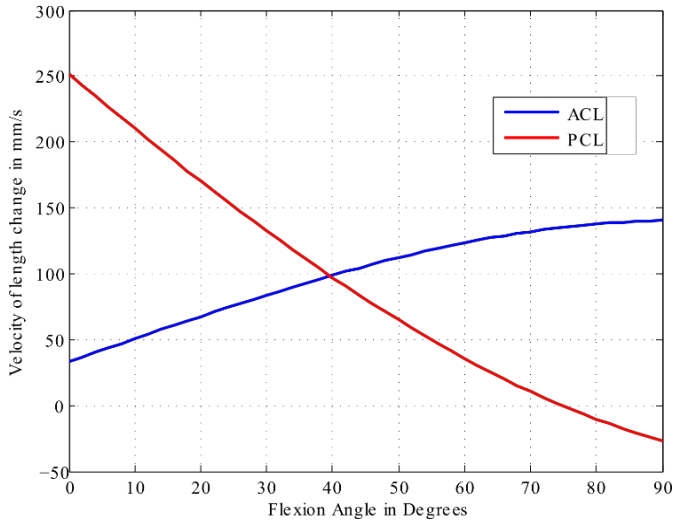


Figure 7. Linear Velocity Profiles of Prosthetic ACL and PCL

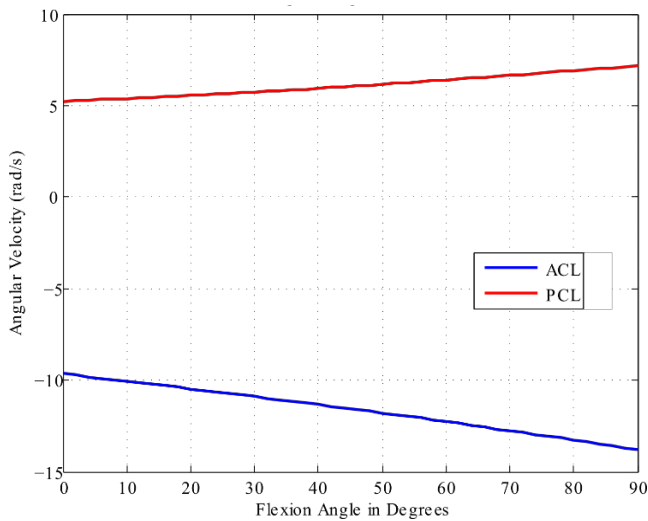


Figure 8. Angular Velocity Profiles of Prosthetic ACL and PCL

Results

Figure 9 shows a single subject fitted with a prosthetic simulator attached to the biomimetic knee to test the knee mechanism. Figure 10 shows the trial being conducted in the Computer Assisted Rehabilitation ENvironment (CAREN) by Motek Medical. The CAREN system is equipped with a Bertec split-belt treadmill, a 6-degree-of-freedom motion base, a 10-camera Vicon motion capture system, Bertec continuous force plates, and a panoramic screen for virtual interaction. The knee's motion was recorded using three reflective markers placed on the prosthesis to obtain the knee angles of the biomimetic knee as the subject walked on the treadmill.



Figure 9. 3D Printed Prosthetic Knee Fitted on the Simulator

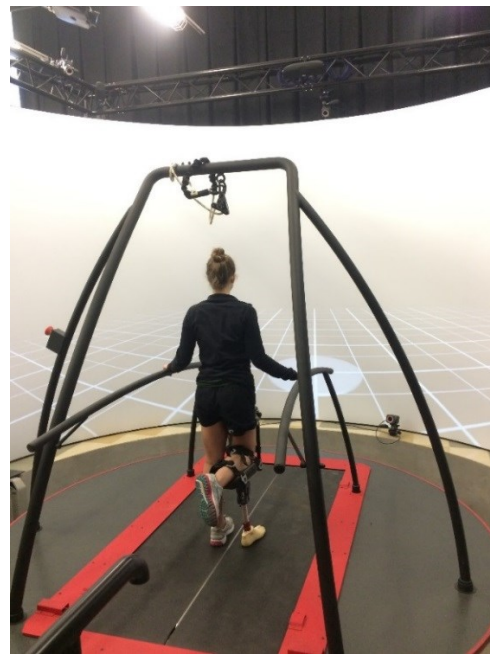


Figure 10. Subject on the CAREN System

The gait data were processed using a Matlab script to calculate the knee angles during gait. The results were compared to the standard able-body knee angle data by Winter [30]. Figure 11 shows the prosthetic gait data obtained with an Ossur Total Knee 2000 with a hydraulic return mechanism obtained by Ramakrishnan et al. [31]. The Biomimetic

knee shows knee angle trends more similar to that of Winter's data than does the Ossur Total knee. This is because the biomimetic knee was designed to have the same dimensions as a human knee and the flexible four-bar mechanism helps in stabilizing the motion. However, there is a clear difference at toe-off between Winter's data and the biomimetic knee, because the biomimetic knee prosthesis is completely passive and, hence, generates less push-off torque. This explains the drop in knee angle just before flexion. The Ossur Total knee has a hydraulic return mechanism and, due to the hydraulic resistance, has a smoother transition from push-off to full flexion [21].

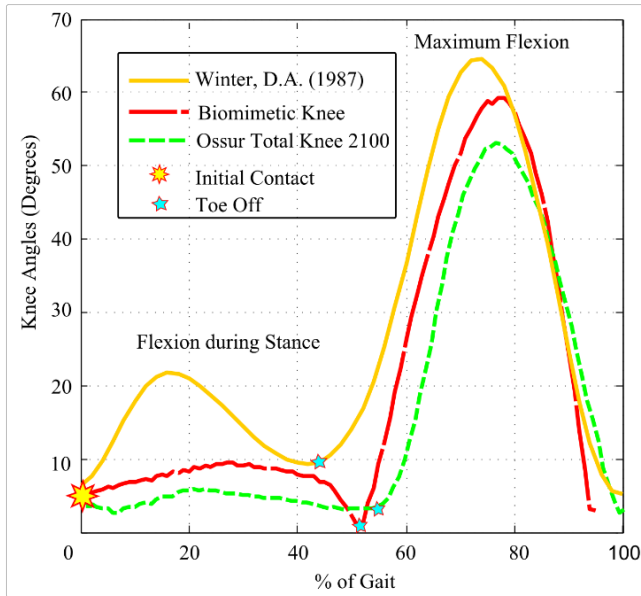


Figure 11. Comparison of Knee Angles

The results of this experiment were obtained using a 3D-printed prototype. The prototype demonstrates the kinematics of the proposed design using the minimum viable product. As stated previously, the kinematics can be tuned to better fit normal human knee motion. This can be done by adjusting the stiffness of the links or by an addition of dampers to make the motion smoother. The knee angles of the two prosthetic knees were compared to published gait data in Figure 11. Figure 12 shows the error between the standard data and the two knees. The average error of the biomimetic knee (6.46°) was lower than the average error of the Ossur Total knee (10.7°). This is because the biomimetic knee uses spring-based, four-bar stabilization, while the Ossur Total knee uses hydraulic resistance that disrupts the natural dynamic motion of the knee by adding excessive damping. This causes lower maximum flexion, as seen in Figure 11. The Ossur knee also had a larger standard deviation error (6.78°) than the biomimetic knee (4.22°).

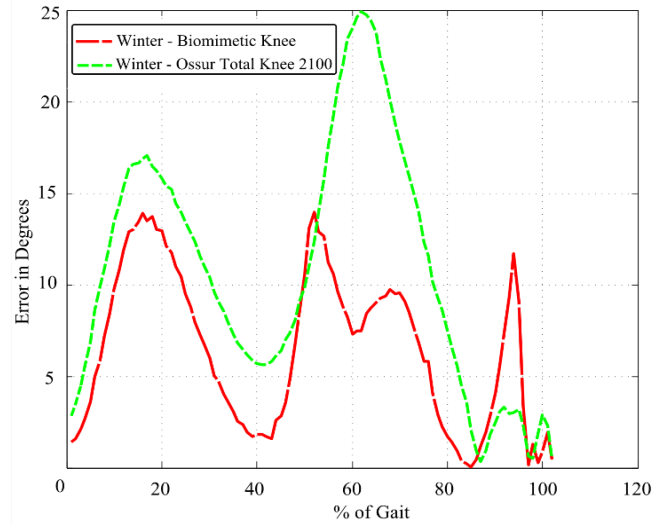


Figure 12. Difference Between Able-Body and Prosthetic Knee Angles

Discussion

This knee design, unlike conventional prosthetic knees, can be scaled to fit any individual, regardless of age, weight, height, or gender. This is because the knee is based on anatomical dimensions and scaling will not affect the function of the mechanism. This design can also be extended into orthotics and humanoid robotics. Orthotics already use similarly geared mechanisms to lock and unlock [32, 33], but the addition of the flexible four-bar links can aid in the stability of the mechanism and can assist the limb to move more like a human knee in the sagittal plane. In humanoid robotics, it could provide the necessary human-like gait motions that are lacking, since most robotic knees are single-axis joints. An actuated version of this mechanism could offer the stability and function that is required by humanoid robots.

This knee mechanism offers the flexibility to design the prosthetic knee to subjective requirements. The designer can start with the condylar measurements obtained from a scan to generate the gear profile. The designer is not constrained to utilize the gear parameters exactly as presented in Table 1. The designer can then model the kinematics of the mechanism to fit the amputee's level of control. This is important because many modern prostheses are rejected by users because the prosthetic components cannot be tuned to their individual specifications [10, 11]. The biomimetic knee prosthetic design has the potential to behave much like an actual human knee in the sagittal plane. The results show that it follows the human knee angle kinematics more closely than does an existing prosthetic knee [31]. The biomimet-

ic knee uses a polycentric mechanism like many popular mechanisms. This offers several advantages compared to a single-axis or simple weight-actuated mechanism, because it helps the shank and foot clear the ground to avoid tripping. In this specific case, the tibia gear rolls on top of the femur gear that helps it move in the vertical direction as well as the horizontal direction, which helps the foot clear the floor during terminal swing phase.

Another major advantage of this design is its ability to be customized. Tuning the prosthetic knee according to a person's body and gait helps in managing their quality of gait [34]. This is important to amputees in order to avoid long-term injuries, due to their physical asymmetry. The process of tuning the prosthesis may be an interesting avenue for future research, because it is important to understand the factors that influence amputee gait. Passive mechanisms such as this can also have simple control systems that may offer long-term benefits to amputees and relieve them from expensive, loud, and inefficient active prosthetic knees. Customization may lead this design to be used by amputees with various levels of control. This is an important factor to address with this knee design, because in current prosthetic technology there are certain types of knees that are designated for each of the K levels. This is a disparate system that can be streamlined with a highly customizable base platform. Further, this design's ability to be scaled to any size will offer better treatment protocols and faster iterations in order to provide the best prosthetic fit for the amputee.

The biomimetic knee described here bridges an important gap in current prosthetic technology trends. This simple design can be mass-produced using both traditional and modern manufacturing processes. This knee is also designed to reduce the cost of manufacturing, since it consists of only two major parts. Further testing is required to evaluate the full capacity of the design. This design can be used with a simple configuration of springs to a more complex fully actuated system for amputees with low muscle control that requires the knee to provide more assistance.

Conclusion

The biomimetic knee design presented here is simple and functional. The assembly consists of the femur gear and tibia gear that are easy to manufacture, which, in turn, will reduce the cost of manufacturing. The rest of the materials can be off-the-shelf components. This, combined with the ability of the design to scale for different amputees, makes this design unique. The results also show that the knee exhibits similar kinematics to the standard human knee model. In future iterations, the knee will be fine-tuned to exhibit more human-like kinematics.

Acknowledgements

This material is based upon work supported by the National Science Foundation under Grant No. MRI-1229561

References

- [1] Perry, J., & Burnfield, J. M. (1992). *Gait Analysis: Normal and Pathological Function*, 271-279.
- [2] Morrison, J. B. (1970). The Mechanics of the Knee Joint in Relation to Normal Walking. *Journal of Biomechanics*, 3(1), 51-61.
- [3] Highsmith, M. J., Kahle, J. T., Bongiorni, D. R., Sutton, B. S., Groer, S., & Kaufman, K. R. (2010). Safety, Energy Efficiency, and Cost Efficacy of the C-Leg for Transfemoral Amputees: A Review of the Literature. *Prosthetics and Orthotics International*, 34(4), 362-377.
- [4] Sup, F., Varol, H. A., Mitchell, J., Withrow, T. J., & Goldfarb, M. (2009). Self-Contained Powered Knee and Ankle Prosthesis: Initial Evaluation on a Transfemoral Amputee. *IEEE International Conference on Rehabilitation Robotics, 2009*, 638-644.
- [5] Sup, F., Bohara, A., & Goldfarb, M. (2008). Design and Control of a Powered Transfemoral Prosthesis. *The International Journal of Robotics Research*, 27(2), 263-273.
- [6] Cantos, M. (2005). *Pirates & Peg Legs: A Historical Look at Amputation and Prosthetics*. History of Medicine Days, 16.
- [7] Childress, D. S. (1985). Historical Aspects of Powered Limb Prostheses. *Clinical Prosthetics & Orthotics*, 9(1), 2-13.
- [8] Highsmith, M. J., Kahle, J. T., Carey, S. L., Lura, D. J., Dubey, R. V., Csavina, K. R., et al. (2011). Kinetic Asymmetry in Transfemoral Amputees While Performing Sit to Stand and Stand to Sit Movements. *Gait & Posture*, 34(1), 86-91.
- [9] Boonstra, A. M., Schrama, J., Fidler, V., & Eisma, W. H. (1995). Energy Cost during Ambulation in Transfemoral Amputees: A Knee Joint with a Mechanical Swing Phase Control vs a Knee Joint with a Pneumatic Swing Phase Control. *Scandinavian Journal of Rehabilitation Medicine*, 27, 77-77.
- [10] Narang, Y. S. (2013). *Identification of Design Requirements for a High-Performance, Low-Cost, Passive Prosthetic Knee through User Analysis and Dynamic Simulation*. Master's thesis, Massachusetts Institute of Technology.
- [11] Goldfarb, M., Lawson, B. E., & Shultz, A. H. (2013). Realizing the Promise of Robotic Leg Prostheses. *Science Translational Medicine*, 5(210), 15.

- [12] Radcliffe, C. W. (1994). Four-Bar Linkage Prosthetic Knee Mechanisms: Kinematics, Alignment and Prescription Criteria. *Prosthetics and Orthotics International*, 18(3), 159-173.
- [13] Michael, J. W. (1999). Modern Prosthetic Knee Mechanisms. *Clinical Orthopaedics and Related Research*, 361, 39-47.
- [14] Shurr, D. G., Michael, J. W., & Cook, T. M. (2002). *Prosthetics and Orthotics*. Prentice Hall.
- [15] Mukul, P., Sadler, J., & Thorsell, E. (2010, May). Stanford-Jaipur Knee Joint for Transfemoral Amputees. *Proceedings of the 13th World Congress of the International Society for Prosthetics and Orthotics*, 1179-80.
- [16] Jin, D., Zhang, R., Dimo, H. O., Wang, R., & Zhang, J. (2003). Kinematic and Dynamic Performance of Prosthetic Knee Joint using Six-Bar Mechanism. *Journal of Rehabilitation Research and Development*, 40(1), 39.
- [17] Ponce-Saldias, D. A., Martins, D., de Mello-Roesler, C. R., Teixeira-Pinto, O., & Fancello, E. A. (2015). Relevance of the Hyperelastic Behavior of Cruciate Ligaments in the Modeling of the Human Knee Joint in Sagittal Plane. *Revista Facultad de Ingenieria Universidad de Antioquia*, 76, 123-133.
- [18] Lührs, B., Theile, F., Griesser, M., Richard, H. A., & Kullmer, G. (2004). U.S. Patent No. 6,749,640. Washington, DC: U.S. Patent and Trademark Office.
- [19] Etoundi, A. C., Burgess, S. C., & Vaidyanathan, R. (2013). A Bio-Inspired Condylar Hinge for Robotic Limbs. *Journal of Mechanisms and Robotics*, 5(3), 031011.
- [20] Zavatsky, A. B., & O'Connor, J. J. (1992). A Model of Human Knee Ligaments in the Sagittal Plane: Part 1: Response to Passive Flexion. *Proceedings of the Institution of Mechanical Engineers, Part H: Journal of Engineering in Medicine*, 206(3), 125-134.
- [21] Hamon, A., Aoustin, Y., & Caro, S. (2014). Two Walking Gaits for a Planar Bipedal Robot Equipped with a Four-Bar Mechanism for the Knee Joint. *Multibody System Dynamics*, 31(3), 283-307.
- [22] Massin, P., & Gournay, A. (2006). Optimization of the Posterior Condylar Offset, Tibial Slope, and Condylar Roll-Back in Total Knee Arthroplasty. *The Journal of Arthroplasty*, 21(6), 889-896.
- [23] Lewek, M., Rudolph, K., Axe, M., & Snyder-Mackler, L. (2002). The Effect of Insufficient Quadriceps Strength on Gait After Anterior Cruciate Ligament Reconstruction. *Clinical Biomechanics*, 17(1), 56-63.
- [24] Siebold, R., Axe, J., Irrgang, J. J., Li, K., Tashman, S., & Fu, F. H. (2010). A Computerized Analysis of Femoral Condyle Radii in ACL Intact and Contralateral ACL Reconstructed Knees Using 3D CT. *Knee surgery, Sports Traumatology, Arthroscopy*, 18(1), 26-31.
- [25] Siu, D., Rudan, J., Wevers, H. W., & Griffiths, P. (1996). Femoral Articular Shape and Geometry: A Three-Dimensional Computerized Analysis of the Knee. *The Journal of Arthroplasty*, 11(2), 166-173.
- [26] Yue, B., Varadarajan, K. M., Ai, S., Tang, T., Rubash, H. E., & Li, G. (2011). Gender Differences in the Knees of Chinese population. *Knee surgery, Sports Traumatology, Arthroscopy*, 19(1), 80-88.
- [27] Monk, A. P., Choji, K., O'Connor, J. J., Goodfellow, J. W., & Murray, D. W. (2014). The Shape of the Distal Femur. *Bone Joint J*, 96(12), 1623-1630.
- [28] Li, G., DeFrate, L. E., Sun, H., & Gill, T. J. (2004). In Vivo Elongation of the Anterior Cruciate Ligament and Posterior Cruciate Ligament during Knee Flexion. *The American Journal of Sports Medicine*, 32(6), 1415-1420.
- [29] McGibbon, C. A. (2012). A Biomechanical Model for Encoding Joint Dynamics: Applications to Transfemoral Prosthesis Control. *Journal of Applied Physiology*, 112(9), 1600-1611.
- [30] Winter, D. A. (1987). *The Biomechanics and Motor Control of Human Gait*, Waterloo.
- [31] Ramakrishnan, T., Muratagic, H., & Reed, K. B. (2016). Combined Gait Asymmetry Metric. *In Engineering in Medicine and Biology Society (EMBC), 2016 IEEE 38th Annual International Conference*, 2165-2168.
- [32] Thompson, J. W. (1978). U.S. Patent No. 4,090,264. Washington, DC: U.S. Patent and Trademark Office.
- [33] Kubein-Meesenburg, D., & Naegerl, H. (2002). U.S. Patent No. 6,443,994. Washington, DC: U.S. Patent and Trademark Office.
- [34] Kark, L., & Simmons, A. (2011). Patient Satisfaction Following Lower-Limb Amputation: the Role of Gait Deviation. *Prosthetics and Orthotics International*, 35(2), 225-233.

Biographies

TYAGI RAMAKRISHNAN is a doctoral candidate in mechanical engineering at the University of South Florida. He earned his BE in Mechanical Engineering from Anna University, Chennai, India, and MSME from the University of South Florida. His interests include biomechanics, human machine interfaces, wearable robotics, and interdisciplinary clinical rehabilitation measures. He may be reached at tyagi@mail.usf.edu

KYLE REED is an associate professor of mechanical engineering at the University of South Florida. He received the BS degree from the University of Tennessee and the MS and PhD degrees from Northwestern University, all in mechanical engineering. He was a postdoctoral fellow in the Laboratory for Computational Sensing and Robotics at the Johns Hopkins University. His interests include haptics, human-machine interaction, rehabilitation, prosthetics, and engineering education. He may be reached at kylereed@usf.edu